

# The Effect of Bone Marrow Derived Mesenchymal Stem Cells on the Ultrastructure of Submandibular Salivary Gland of Induced Hypothyroidism in Rats (Electron Microscopic Study)

Original  
Article

Dina Maged Eldahrawy<sup>1</sup>, Heba A. Adawy<sup>2</sup>, Mona Fathy El Deeb<sup>1</sup>

<sup>1</sup>Department of Oral Biology, Faculty of Oral and Dental Medicine, Future University in Egypt

<sup>2</sup>Department of Oral and Dental Biology, Faculty of Dental Medicine for Girls, AL-Azhar University, Egypt

## ABSTRACT

**Background:** Hypothyroidism is a clinical disorder that results from insufficient production of thyroid hormones leading to a total decrease of metabolic demands of the body and causing serious abnormalities. Hypothyroidism is known to affect salivary glands causing deleterious changes including apoptosis and numerous cytoplasmic vacuolation. Mesenchymal stem cells (MSCs) have high capability of self-renewal. Thus, have enormous therapeutic potential for tissue repair.

**Objective:** The study aimed to assess the influence of bone marrow derived mesenchymal stem cells (BM-MSCs) on the histological ultrastructure of submandibular salivary gland of carbimazole-induced hypothyroidism in rats.

**Method:** Twenty one adult male albino rats were divided into three groups (seven rats each). Group I: Is considered as control group. Group II: (Carbimazole induced hypothyroidism group): animals were given a single daily oral dose of carbimazole (5mg/250g/day) dissolved in 3 ml of distilled water delivered by intragastric tube for five weeks, to induce hypothyroidism. Group III: (BM-MSCs treated group): hypothyroidism was induced similar to group II. Then rats were injected at the lateral tail vein with  $1 \times 10^7$  BM-MSCs cells in 0.2ml phosphate buffer saline immediately following induction of hypothyroidism. All rats were euthanized after 8 weeks (5 weeks of hypothyroidism induction + 3 weeks of stem cells injection). Submandibular salivary glands were prepared for transmission electron microscopic examination (TEM).

**Results:** Ultrastructural results of group II revealed massive degenerative changes within the acinar and ductal cells' nuclei and organelles, together with disruption of their intercellular junctions. Marked improvement of parenchymal cells' architecture was detected with BM-MSCs administration in group III.

**Conclusion:** BM-MSCs have the potentiality to repair salivary glands damage following induction of hypothyroidism.

**Received:** 12 February 2021, **Accepted:** 22 March 2021

**Key Words:** Bone marrow derived mesenchymal stem cells (BM-MSCs), carbimazole, hypothyroidism, submandibular salivary gland.

**Corresponding Author:** Mona Fathy El Deeb, PhD, Department of Oral Biology, Faculty of Oral and Dental Medicine, Future University in Egypt, **Tel.:** +20 10050 00490, **E-mail:** mona.eldeeb@fue.edu.eg

**ISSN:** 1110-0559, Vol. 45, No.2

## INTRODUCTION

Hypothyroidism is a condition in which thyroid hormones production decreases below the standard level. It results from thyroid disorder, impairment in the mechanisms controlling the formation of these hormones, or may arise from complications while treating hyperthyroidism<sup>[1]</sup>.

Oral manifestations of hypothyroidism appear in the form of enlarged tongue and increased susceptibility to dental caries. The salivary glands may also be enlarged, which may help in the diagnosis of hypothyroid cases<sup>[2]</sup>. Moreover, submandibular salivary gland is well known to be a target organ for thyroid hormones. Hypothyroidism results in acinar alterations showing apoptosis, and numerous cytoplasmic vacuolation<sup>[3]</sup>.

Mesenchymal stem cells (MSCs) are undifferentiated cells capable of self-renewal. They are found in mesenchymal tissues as well as bone marrow. These

cells are able to differentiate into non-mesodermal cells, myocytes, adipocytes, chondrocytes and osteoblasts<sup>[4]</sup>. They have effective regenerative role in maxillofacial region such as periodontal ligament, pulp, teeth and salivary glands repair. They have been also used in reconstruction of enamel and dentin, and in repair of cleft lip and palate<sup>[5]</sup>.

MSCs exhibit enormous healing capacity for tissue repair. For now, salivary glands' structure was almost restored after bone marrow derived mesenchymal stem cells (BM-MSCs) transplantation following radiotherapy<sup>[6]</sup>. Moreover, authors spotted that BM-MSCs were able to reduce radiation induced mucositis in tongue of albino rats<sup>[7]</sup>. Previous study revealed that wounds treated with BM-MSCs lead to acceleration of re-epithelization, angiogenesis and granulation tissue formation in rats<sup>[8]</sup>. In addition, BM-MSCs was found to have curative effect on induced oral ulcers in rats<sup>[9]</sup>.

Accordingly, it is hypothesized that systemic administration of BM-MSCs could be beneficial in improving the drawbacks on the submandibular salivary glands resulting from drug induced hypothyroidism. Hence, the purpose of this research was to assess the effect of BM-MSCs on the histological structure of submandibular salivary gland of carbimazole-induced hypothyroidism in rats through transmission electron microscopic (TEM) examination.

## MATERIALS AND METHODS

### Materials

- Carbimazole 5mg was purchased from “Chemical Industries Development, Giza, A.R.E”. It was supplied as tablets having the trade name (Carbimazole)
- BM-MSCs were obtained from “Biochemistry Department”, Faculty of Medicine, Cairo University

### Animals

Twenty one adult male albino rats were used in this study weighing between 200-250 grams. The rats were housed in the animal house of Faculty of Medicine, Cairo University. Animals were housed under measured humidity, temperature, and dark-light cycle. They were allowed to access freely adequate balanced diet and fresh water. The experiment was supervised by a specialized veterinarian throughout the experimental period.

### Study design

The design of the study was permitted by the ethical committee of AL-Azhar University (REC18-082).

After one week acclimatization period, the animals were randomly divided into three groups (seven rats each):

**Group I (Control group):** Rats of this group were allowed to access freely balanced diet and freshwater supply throughout the experimental period.

**Group II (Carbimazole induced hypothyroidism group):** For induction of hypothyroidism, rats were given a single daily dose of carbimazole (5mg/250g/day) dissolved in 3 ml of distilled water and delivered orally by intragastric tube for 35 successive days (5 weeks)<sup>[10]</sup>.

To confirm induction of hypothyroidism, blood samples were collected from retro orbital veins after five weeks from the beginning of carbimazole treatment for measurement of serum T3 and T4<sup>[11]</sup> (Table 1). Blood samples were also collected from this group every week throughout the remaining experimental period to ensure continuation of the hypothyroid state.

**Table 1:** Showing the mean of serum T3 and T4 of hypothyroid rats compared to the reference value of normal rats

Test	Hypothyroid group	Reference value
Serum T3	99 ng/dl	205-269 ng/dl
Serum T4	4.08 $\mu$ g/dl	7.3-15 $\mu$ g/dl

**Group III (BM-MSCs treated group):** Hypothyroidism was induced in rats of this group similar to group II. Then rats were injected at the lateral tail vein with  $1 \times 10^7$  BM-MSCs cells in 0.2ml phosphate buffer saline (PBS)<sup>[12]</sup> immediately following induction of hypothyroidism (after 5 weeks).

Three weeks after stem cells injection, rats of all groups were euthanized by an intraperitoneal overdose of sodium thiopental (80 mg/ kg). Thus the total experimental period will be 8 weeks; (5 weeks of hypothyroidism induction + 3 weeks of stem cells injection).

### Preparation of BM-MSC stem cells

Isolation of BM-MSCs from the femurs and tibiae of male albino rats then labeling using PKH26 fluorescent linker dye for cell tracking, were performed in the “Biochemistry Department”, Faculty of Medicine, Cairo University. At the endpoint of the study, the submandibular gland was examined using florescent microscopy to trace the stained cells with the dye, so to confirm engraftment of these cells into the hypothyroid rats’ gland (Figure 1).

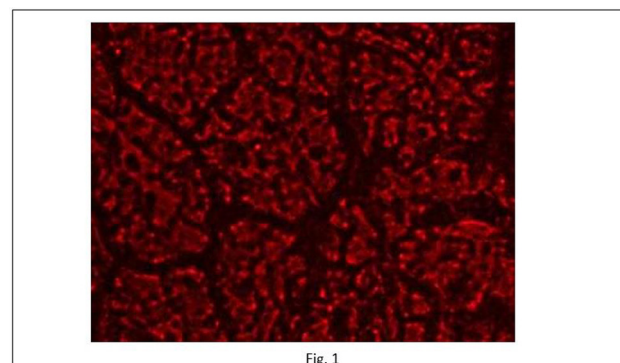


**Fig. 1:** Photomicrograph of group III showing detected BM-MSCs labeled with red fluorescent PKH26 dye in whole submandibular salivary gland tissue (PKH26, Original Mag.  $\times 200$ )

### Methods of investigation

After euthanization, the submandibular salivary glands from both sides were immediately dissected and prepared for TEM examination.

### Sample preparation for transmission electron microscope (TEM)

Small parts from the dissected submandibular gland (1-3mm) size were thoroughly washed in PBS (pH 7.4). They were placed in Karnovsky’s fixative (2.5 % glutaraldehyde and 2 % paraformaldehyde in 0.1 M PBS for 8-12 hrs.). Samples were fixed again in 2 % osmium tetroxide for 2 hrs. Tissues were then dehydrated, cleared, infiltrated, embedded, finally polymerized.

Semi thin sections (0.5-1  $\mu$ ) were produced using LKB ultra microtome. Following, staining with toluidine blue was done and samples were inspected under light microscopy. Ultrathin sections (70-90 nm) were performed on copper grids and contrasted using uranyl acetate

(for 15 min) and lead citrate (for 10 min)<sup>[13]</sup>. Lastly, specimens were photographed by TEM (Jeol JEM-100CX II EM) in the Electron Microscopy Unit, Al-Azhar University.

## RESULTS

---

Before dissection, the gross picture of the submandibular salivary gland appeared normal with no detected alterations.

### *Control group (group I)*

#### *\*Acinar cells*

Parenchymal cells of the submandibular salivary gland showed basal spheroidal nuclei with regular outline and homogeneously distributed chromatin displaying granular appearance, and prominent nucleoli. Parallel aggregations of rough endoplasmic reticulum (RER) appeared basal to the nucleus together with few oval mitochondria with transverse cristae. In addition, varying electron density and size of membrane bounded secretory granules were observed surrounding the nucleus (Figure 2).

#### *\*Intercalated duct*

The intercalated duct cells exhibited large centrally placed nucleus occupying most of the cell. Moreover, few normally appearing cisternae of RER and secretory granules together with scattered mitochondria were also encountered in the cytoplasm. On the other hand, normal desmosomal junctions were recognized throughout the boundaries of the cells (Figure 3).

#### *\*Striated duct*

Striated duct cells revealed numerous apical microvilli. The cells showed large central oval nuclei with granular appearance bounded by few RER. Basally, the cells exhibited parallel plasma membrane infoldings containing abundant rod shaped mitochondria with palisading arrangement. Desmosomal junctions were clearly detected between striated ductal cells (Figure 4).

#### *\*Granular convoluted tubules*

The basal part of the granular convoluted tubule (GCT) cells contained rounded, regular outlined nucleus with prominent nucleolus. The nucleus was bounded by abundant mitochondria at the vicinity of the basal plasma membrane, together with few cisternae of RER. Multiple membrane bounded granules of varying size and density filled the apical two third of the cells. Junctional complexes were also recognized between the basal plasma membrane of GCT cells (Figure 5).

#### *\*Excretory duct*

The excretory duct cells exhibited normally appearing nucleus with homogeneously distributed chromatin, abundant mitochondria and scanty RER. Cells also presented microvilli on their luminal boundaries, and numerous desmosomal junctions on their lateral margins. (Figure 6).

### *Carbimazole induced Hypothyroidism group (group II)*

In group II, massive degenerative alterations were detected within all parenchymal elements of the submandibular salivary gland.

#### *\*Acinar cells*

TEM of group II showed obvious acinar cellular damage. Some nuclei showed early apoptotic changes as irregularity of the nuclear membrane and chromatin clumping. Also, dilatation of the nuclear membrane with existence of perinuclear halo was also a detectable feature. Some nuclei appeared pyknotic and shrunken with chromatin condensation. The RER presented variable changes ranging from dilatation and widening of cisternal spaces, to discontinuity and fragmentation exhibiting granular appearance. Dilated mitochondria with disrupted cristae were also marked in the acinar cells. Moreover, secretory granules showed apparent reduction with variable electron densities and ill-defined outlines. Areas of vacuolar degeneration were also spotted within the acinar cytoplasm (Figure 7).

#### *\*Intercalated duct*

Some nuclei of the intercalated duct cells appeared closed faced with chromatin condensation, others were shrunken and pyknotic. Moreover, the RER showed moderate dilatation, while the mitochondria appeared elongated with partial loss of their cristae. On the other hand, marked loss of attachment between ductal cells was clearly evident (Figure 8).

#### *\*Striated duct*

Irregular orientation of basal plasma membrane infolding in the striated duct cells was recognized. Some nuclei showed signs of degeneration presented by nuclear membrane irregularity and pyknosis. The mitochondria were highly affected in which some appeared dense and elongated between the collapsed membrane infoldings, while others were markedly distended with massive disruption of their cristae. The RER were sparse, disrupted, severely diminished and abnormally dilated. Moreover, the cytoplasm showed extensive areas of vacuolar degeneration. Besides, the desmosomal junctions were distorted at the apical area between the cells (Figure 9).

#### *\*Granular convoluted tubules*

Ultrastructure examination of GCTs showed some cells with few electron dense secretory granules surrounded by cytoplasmic vacuolation. Numerous swollen and degenerated mitochondria with damaged cristae were encountered together with scanty and dilated sacs of RER. Meanwhile, massive areas of vacuolar degeneration were obviously found throughout the cytoplasm (Figure 10).

#### *\*Excretory duct*

Excretory duct lining cells revealed apical shrunken

nuclei. Moreover, mitochondrial degeneration was evident with dilated, granular RER and few vacuolated areas. Loss of attachment between cellular boundaries was also recognized apically (Figure 11).

### ***BM-MSCs treated group (group III)***

In this group, all parenchymal elements showed marked ultrastructural improvement of their acini and ducts to a great extent approaching those of the control group.

#### ***\*Acinar cells***

In this group, the nucleus appeared normally rounded with well-defined nuclear membrane and homogeneously distributed peripheral chromatin. Prominent nucleolus could be detected as well. The RER was relatively well organized and arranged in parallel rows with few areas of persistent dilatation. Meanwhile, normally appearing mitochondria were recognized, while few expressed partial loss of their cristae (Figure 12).

#### ***\*Intercalated duct***

Intercalated ducts cells showed regain of normal nuclear appearance. Uniform arrangement of cisternae of RER was spotted with slight dilatation together with normally appearing mitochondria. Besides, few well defined electron dense secretory granules could also be observed at the apical part of the ductal cells. Furthermore, cells had no disruption of their intercellular junctions (Figure 13).

#### ***\*Striated duct***

The basal folding of plasma membrane regained its uniform arrangement in radial pattern with elongated and numerous longitudinally oriented mitochondria. Moreover, scanty RER and few areas of cytoplasmic vacuolation were hardly detected. As well, desmosomal junctions between the cells were clearly distinguishable with no intercellular spaces (Figure 14).

#### ***\*Granular convoluted tubules***

GCT cells appeared studded with electron dense secretory granules. The nucleus appeared normal as well the RER which assumed normal configuration with scanty areas of distended cisternae. Moreover, mitochondria were scanty exhibiting transverse cristae. Normal intercellular junctions could also be detected between GCT cells (Figure 15).

#### ***\*Excretory duct***

Normal nucleus as well as numerous normal mitochondria and few distended RER were spotted within the excretory duct cells. Moreover, no disruption of intercellular junctions was recognized between excretory duct cells (Figure 16).

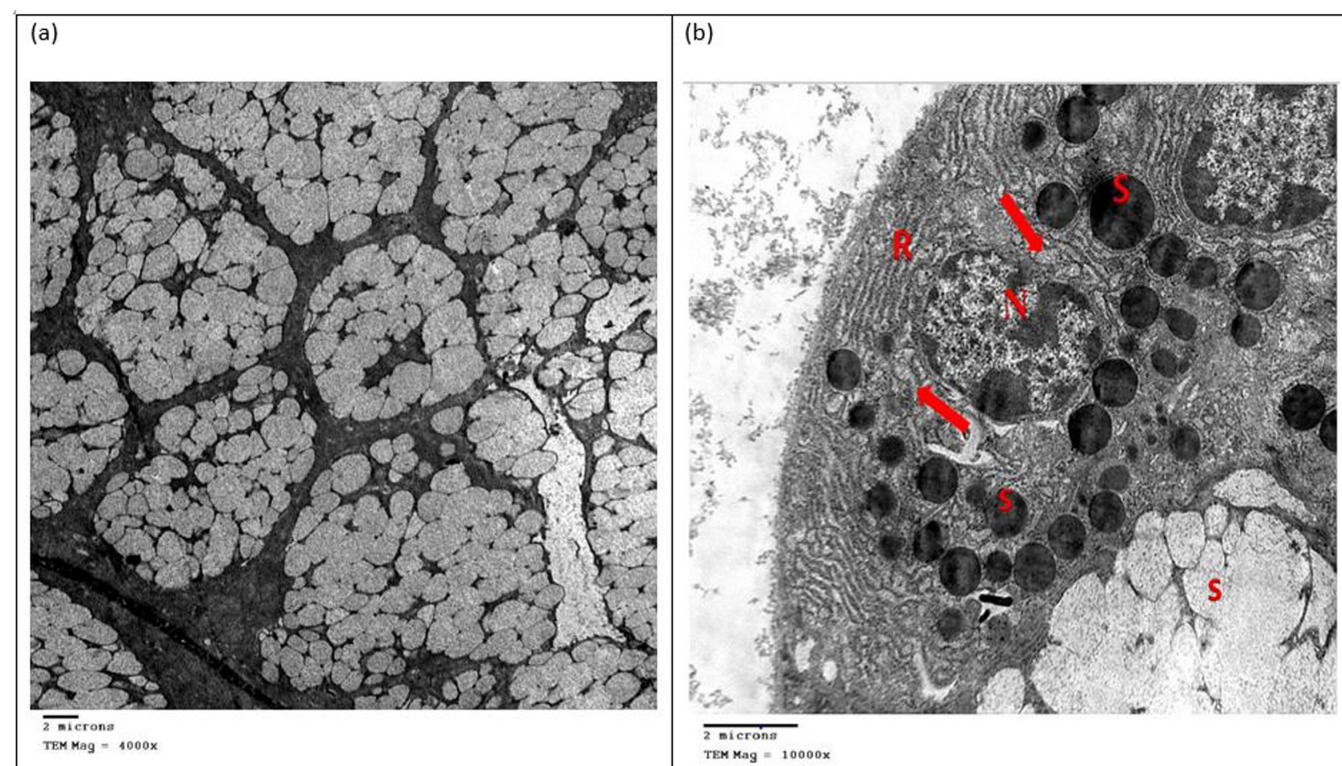


**Fig. 2:** Electron micrograph of acini of submandibular salivary gland of group I showing: [a] acinar cells [b] regular nucleus with prominent nucleolus (N), parallel arrays of RER (R), mitochondria with transverse cristae (red arrows), secretory granules of variable densities (S) (Uranyl acetate and lead citrate [a] x4000 [b] x10000).

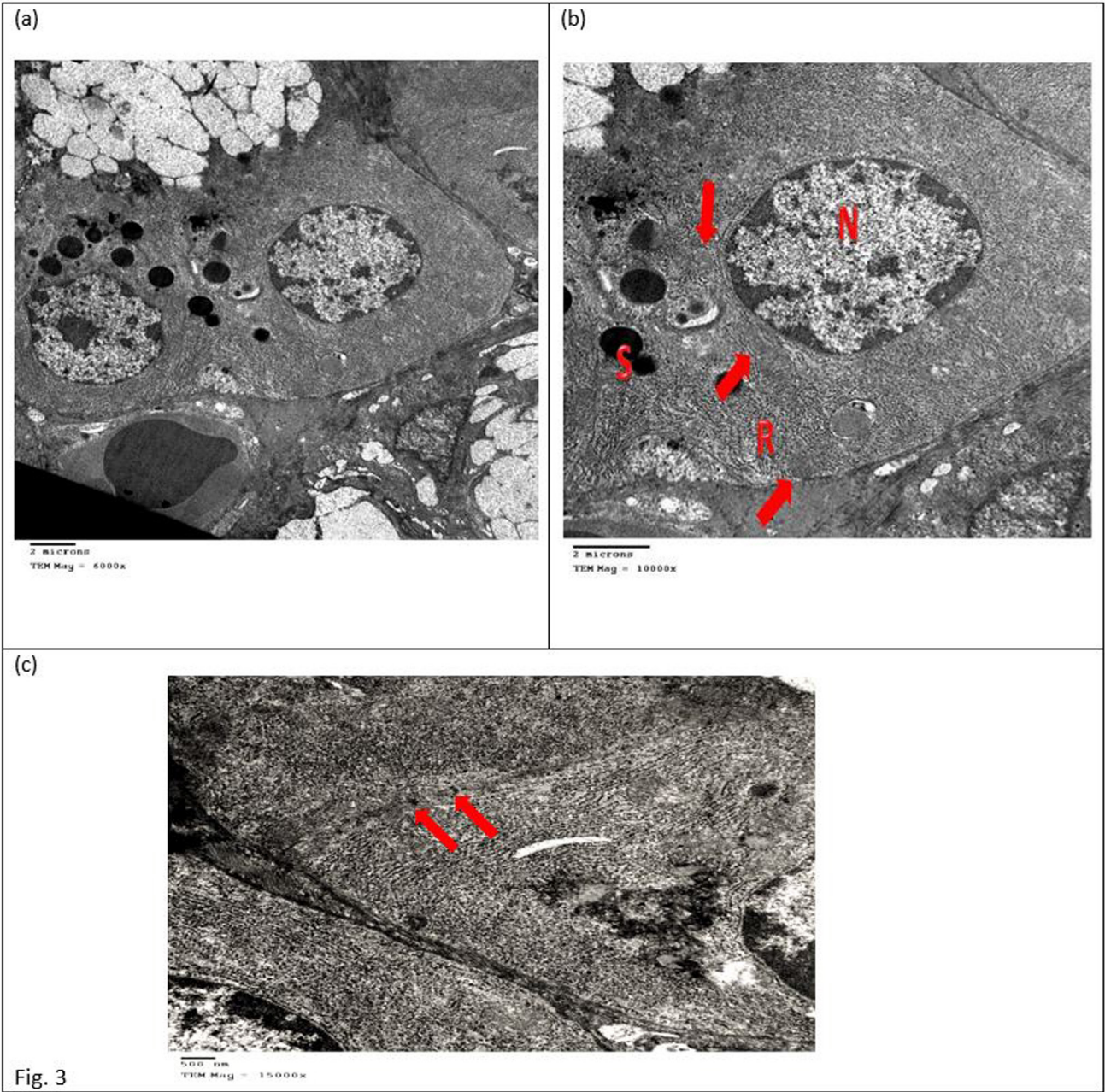


**Fig. 3:** Electron micrograph of intercalated duct of submandibular salivary gland of group I showing: [a] intercalated duct cells [b] large central nucleus (N), few RER (R), scattered mitochondria (red arrows), few secretory granules (s). [c] normal desmosomal junctions (red arrows) (Uranyl acetate and lead citrate [a] x6000 [b] x10000 [c] x15000).

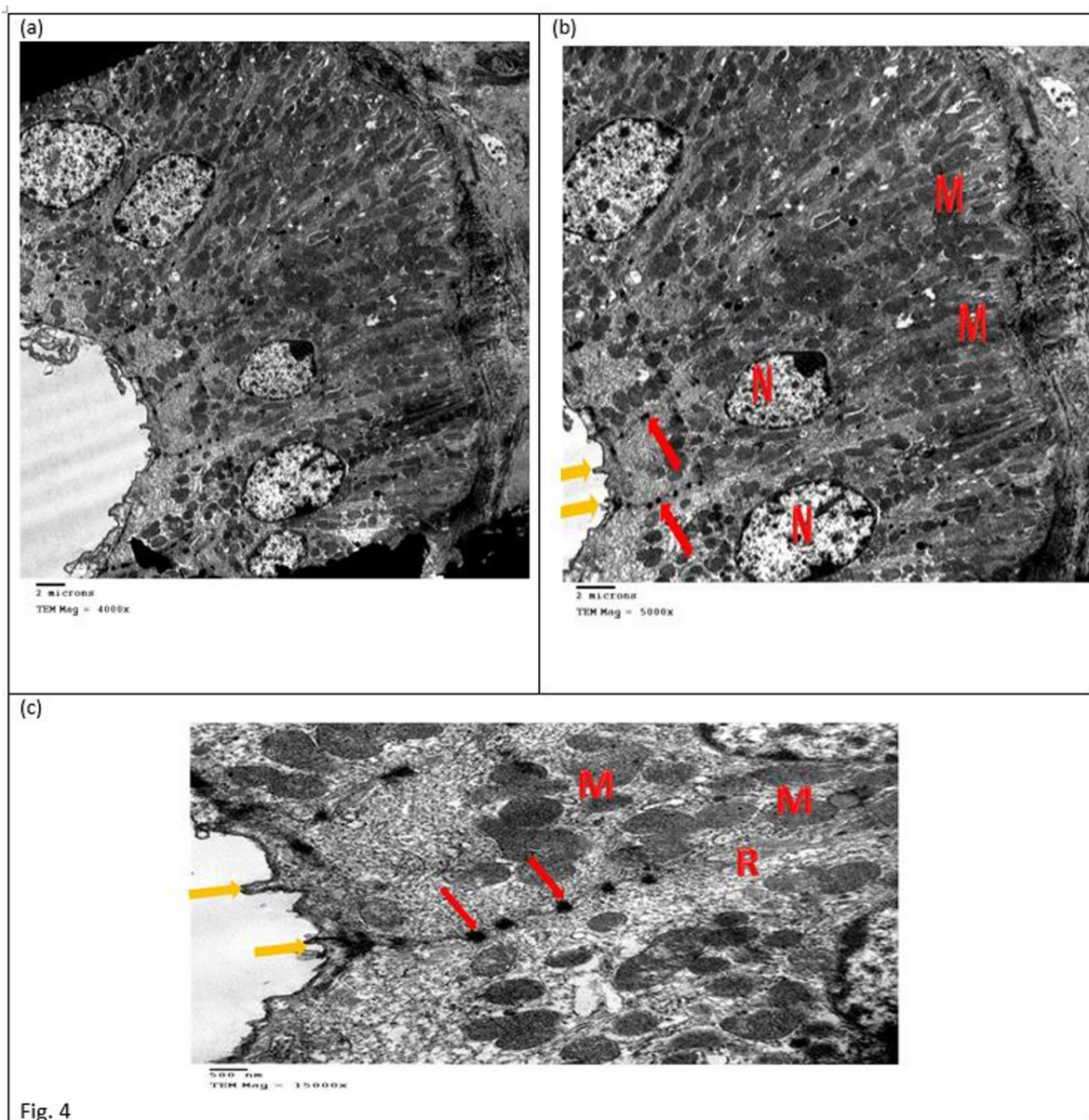
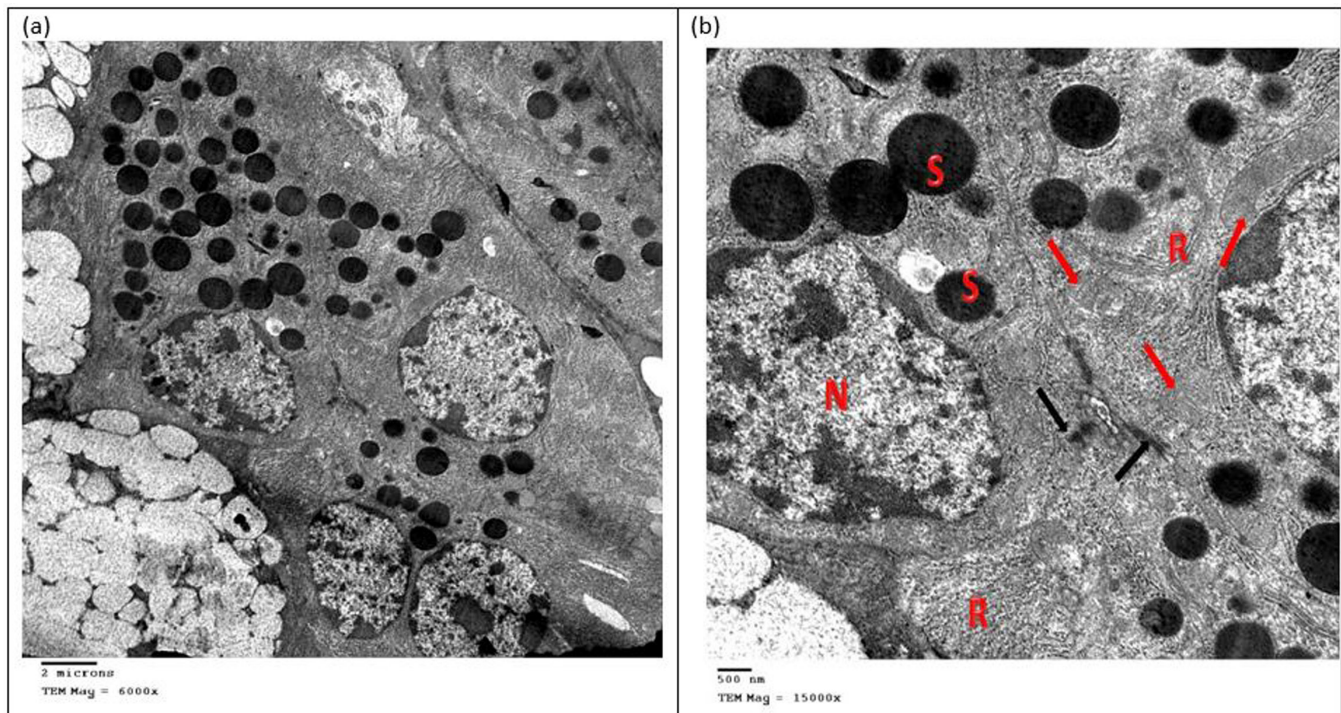
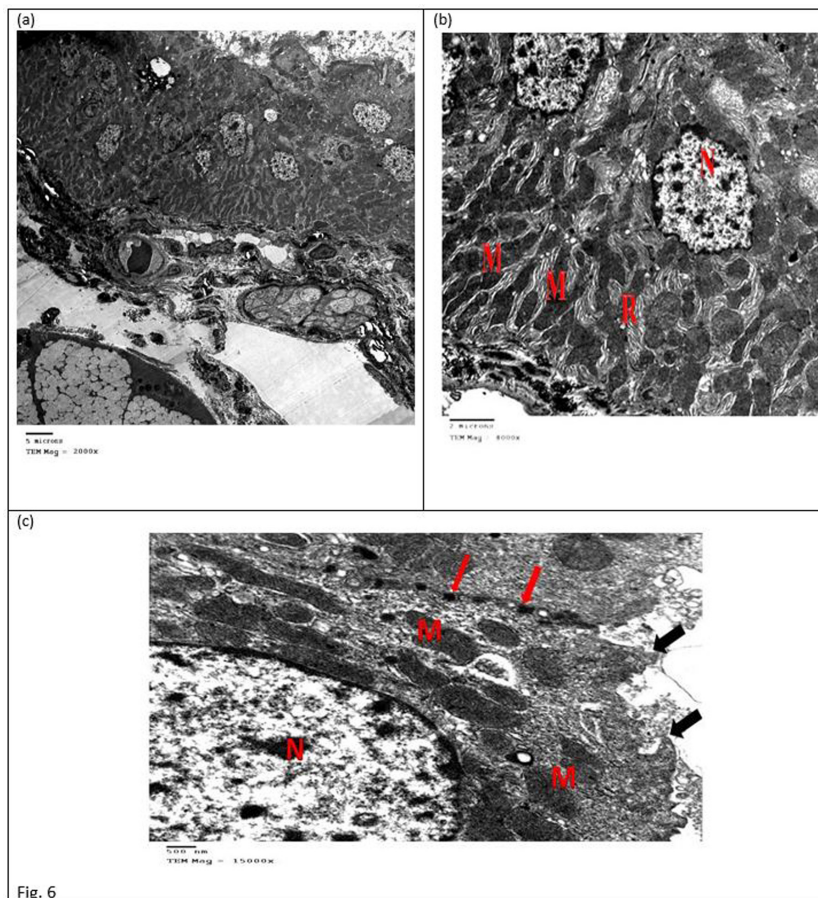


Fig. 4

**Fig. 4:** Electron micrograph of striated duct of submandibular salivary gland of group I showing: [a] striated duct cells [b] large oval nucleus (N), apical microvilli (yellow arrows), palisading arrangement of mitochondria (M), normal desmosomal junction (red arrows) [c]: numerous mitochondria (M), few RER (R), desmosomal junctions (red arrows), apical microvilli (yellow arrows) (Uranyl acetate and lead citrate [a]x4000 [b] x5000 [c] x15000).



**Fig. 5:** Electron micrograph of GCT of submandibular salivary gland of group I showing: [a] GCT cells [b] the nucleus (N), mitochondria (red arrows), numerous secretory granules (S), RER (R), desmosomal junctions (black arrows) (Uranyl acetate and lead citrate [a] x6000 [b] x15000).



**Fig. 6:** Electron micrograph of excretory duct of submandibular salivary gland of group I showing: [a] excretory duct cells [b] slightly irregular nucleus (N), abundant mitochondria (M), scanty RER (R) [c] nucleus (N), abundant mitochondria (M), numerous desmosomal junctions (red arrows) microvilli (black arrows) (Uranyl acetate and lead citrate [a] x2000 [b] x8000 [c] x15000).

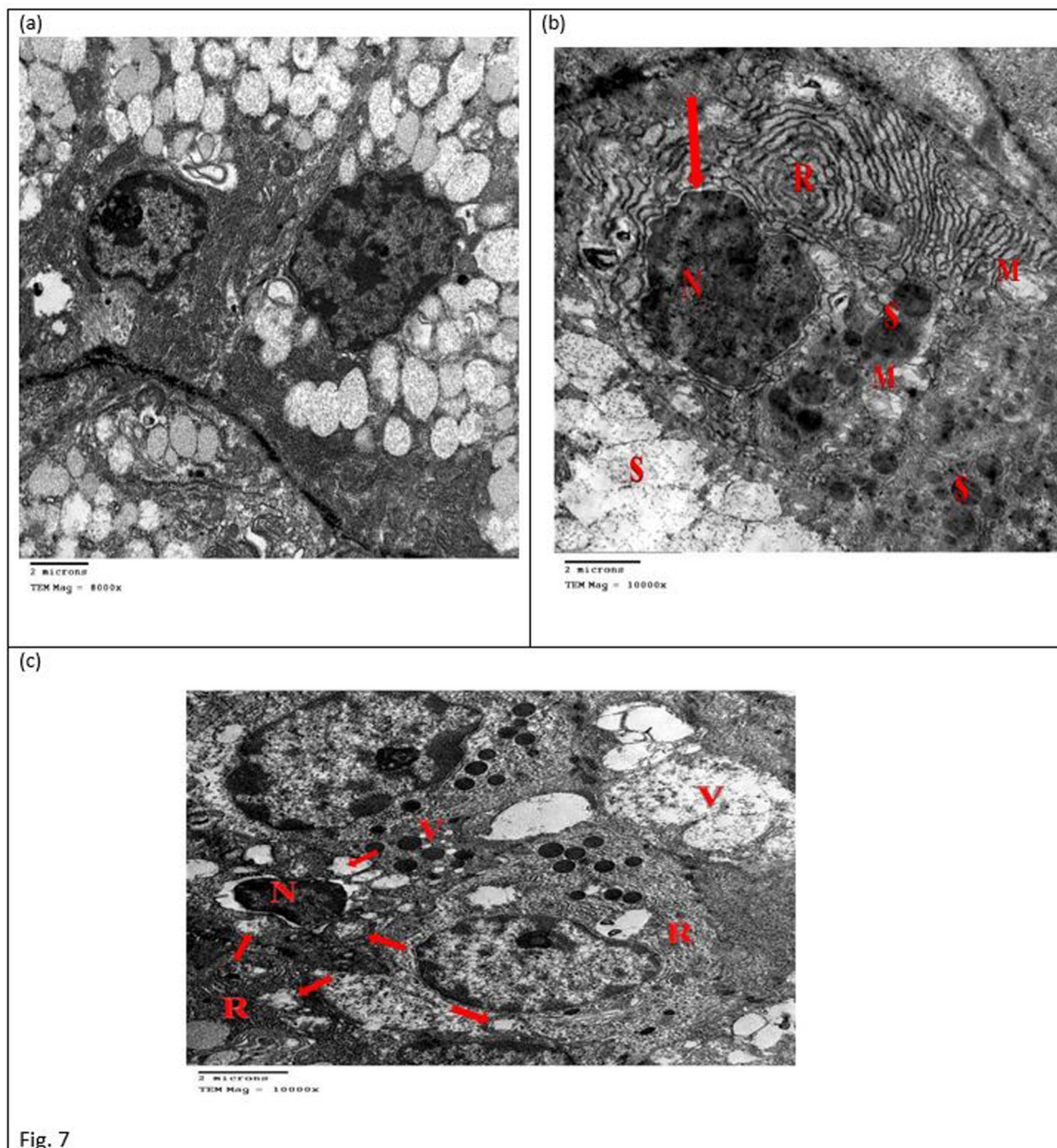


**Fig. 7:** Electron micrograph of acini of submandibular salivary gland of group II showing: [a] acinar cells [b] hyperchromatic nucleus (N) with dilated perinuclear membrane and irregular nuclear margin (red arrow), dilated RER with wide cisternal spaces (R), dilated mitochondria with partially disrupted cristae (M), ill-defined secretory granules with variable densities (s) (Uranyl acetate and lead citrate x10000) [c] pyknotic shrunken nucleus (N), dilated mitochondria with partial loss of cristae (red arrows), RER exhibiting granular appearance (R), numerous vacuolation (V) (Uranyl acetate and lead citrate [a] x8000 [b] & [c] x10000).

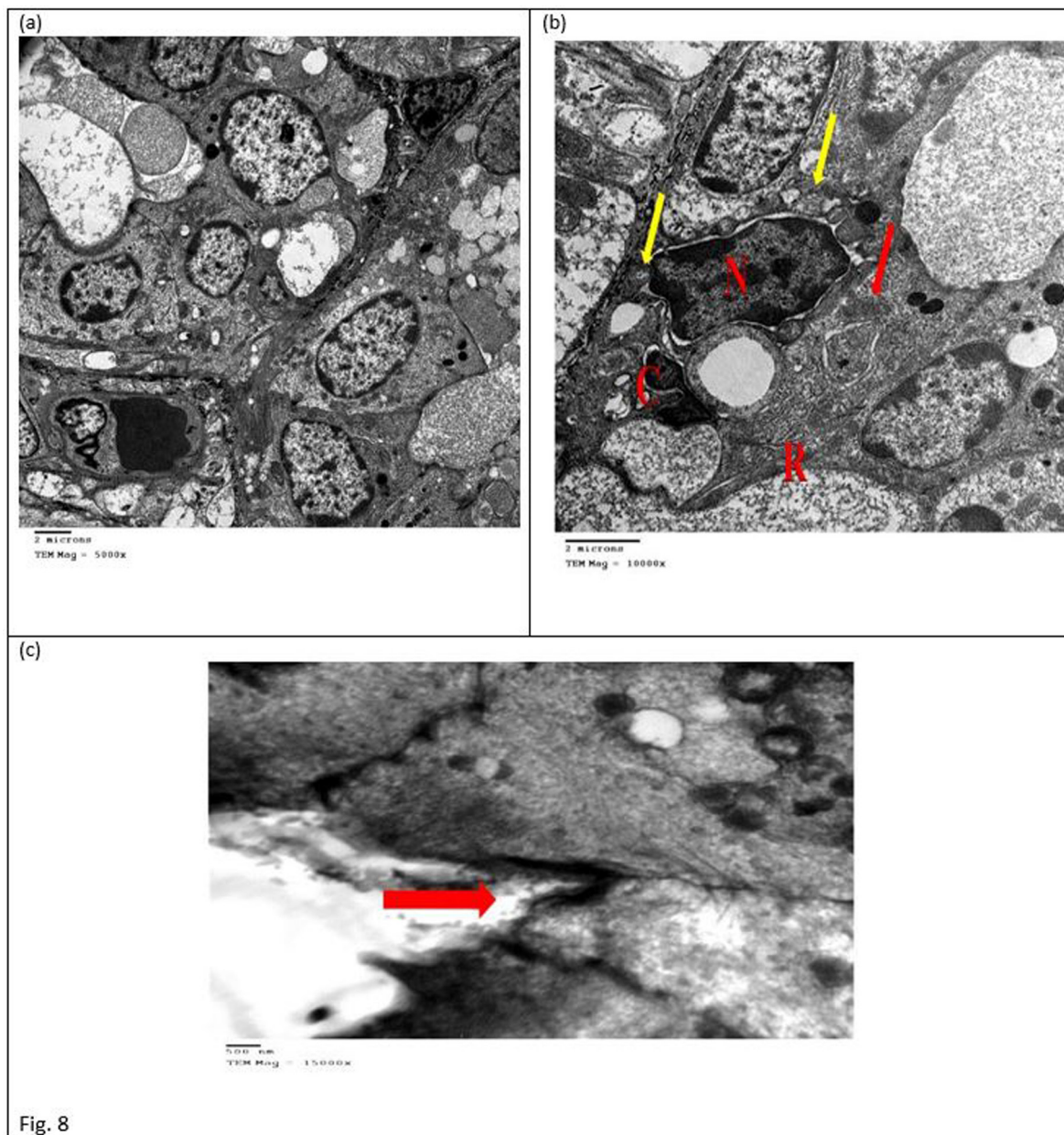
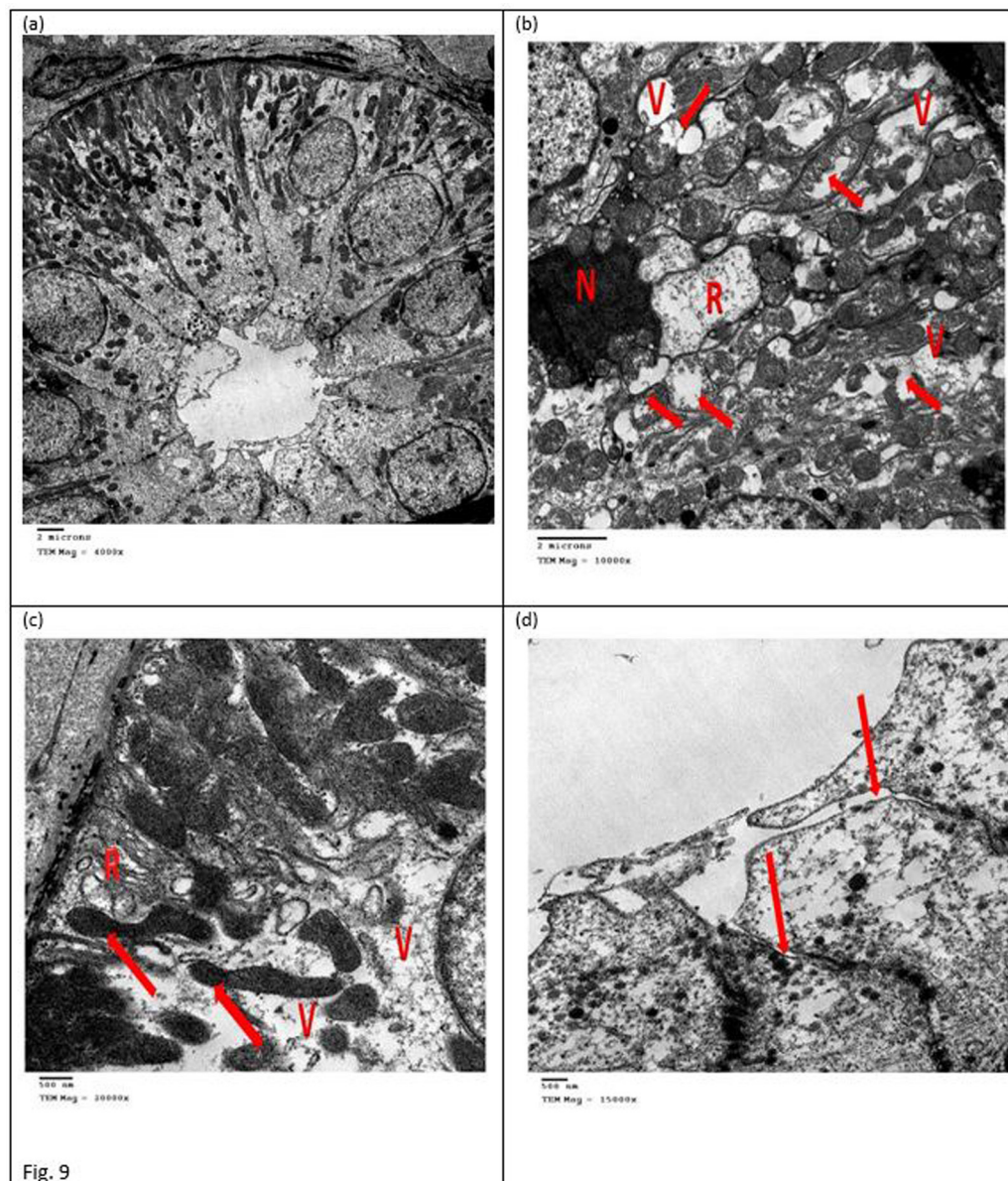
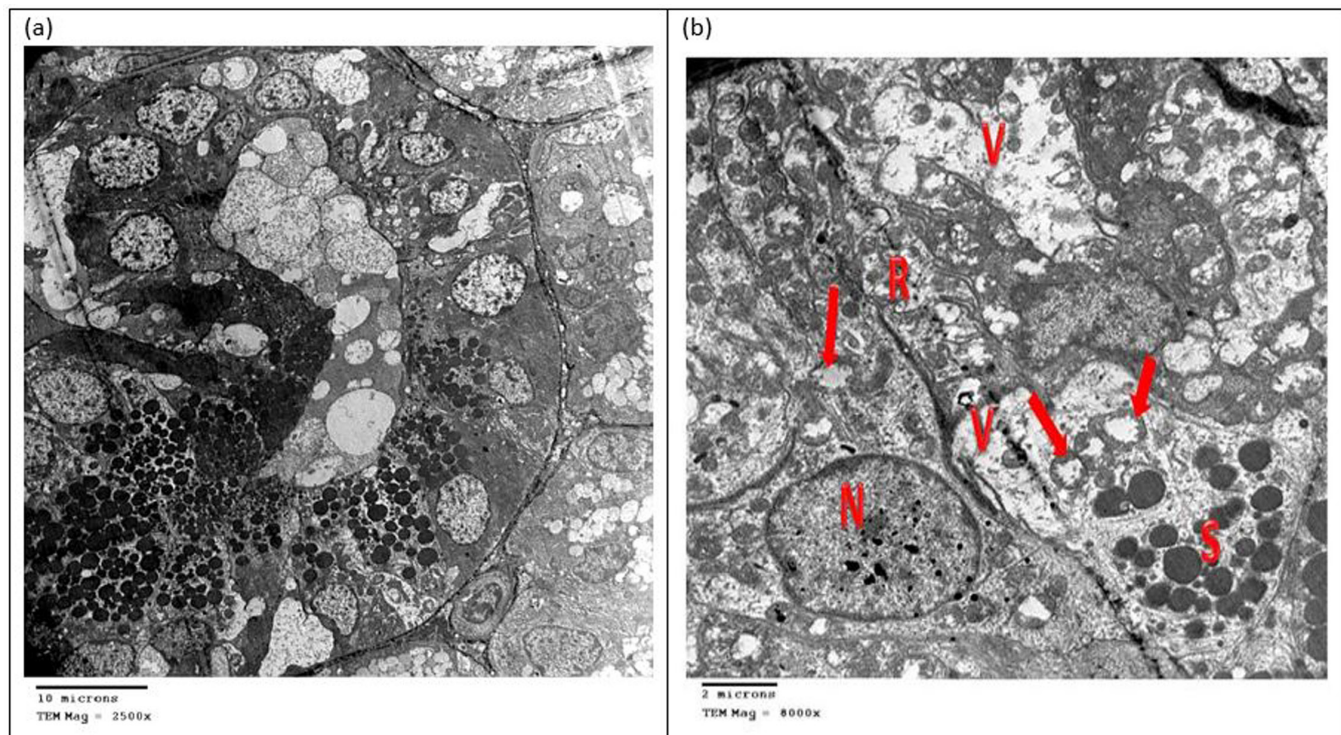


Fig. 8

**Fig. 8:** Electron micrograph of intercalated duct of submandibular salivary gland of group II showing: [a] intercalated duct cells [b] closed faced nucleus (N), pyknotic nucleus (C) elongated mitochondria (red arrow), partial loss of cristae (yellow arrows), moderate dilatation of RER (R) [c] loss of attachment between the cells (red arrow) (Uranyl acetate and lead citrate [a] x5000 [b] x10000 [c] x15000).



**Fig. 9:** Electron micrograph of striated duct of submandibular salivary gland of group II showing: [a] striated duct cells [b] pyknotic nucleus with irregular nuclear membrane (N), distended mitochondria with massive loss of cristae (red arrows), extensive vacuolation (V), abnormally dilated RER(R) [c] dense and elongated mitochondria (red arrows), disrupted and dilated sacs of RER (R), extensive vacuolar degeneration (V) [d] loss of attachment between the cells at the apical area (red arrows) (Uranyl acetate and lead citrate [a] x4000 [b] x10000 [c] x20000 [d] x15000).



**Fig. 10:** Electron micrograph of GCT of submandibular salivary gland of group II showing: [a] GCT cells [b] nucleus (N), few electron dense secretory granules (s), swollen and degenerated mitochondria (red arrows), scanty and dilated RER (R), massive vacuolated areas (V) (Uranyl acetate and lead citrate [a] x2500 [b] x8000).

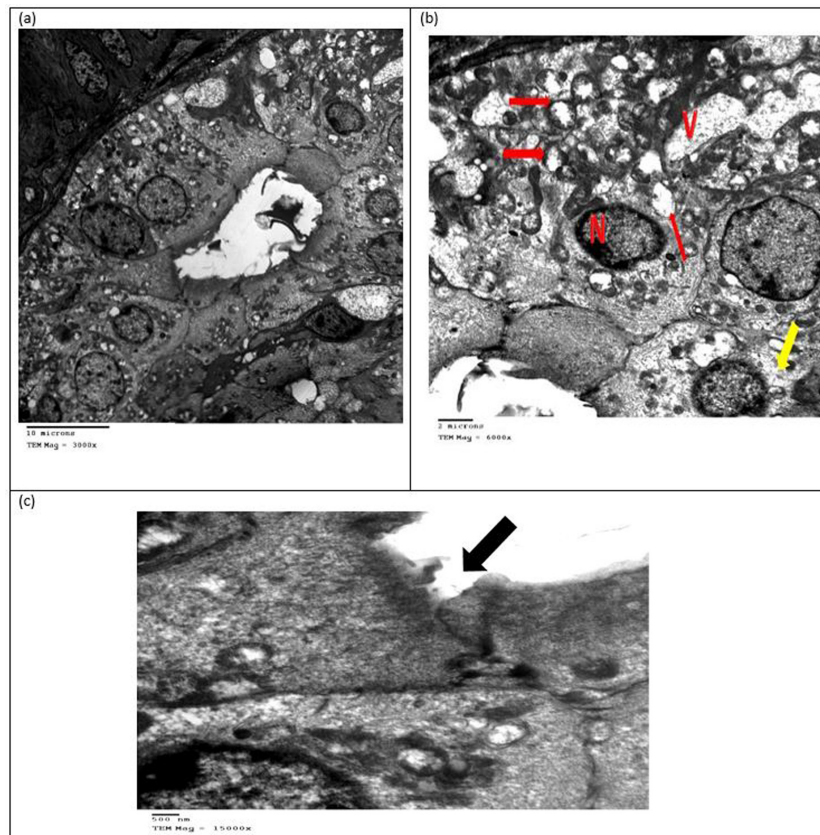


**Fig. 11:** Electron micrograph of excretory duct of submandibular salivary gland of group II showing: [a] excretory duct cells [b] shrunken apically displaced nucleus (N), degenerated mitochondria (red arrows), dilated granular RER (yellow arrow), vacuolar degeneration (V) [c] loss of cellular attachment (black arrow) (Uranyl acetate and lead citrate [a] x3000 [b] x 6000 [c] x15000).

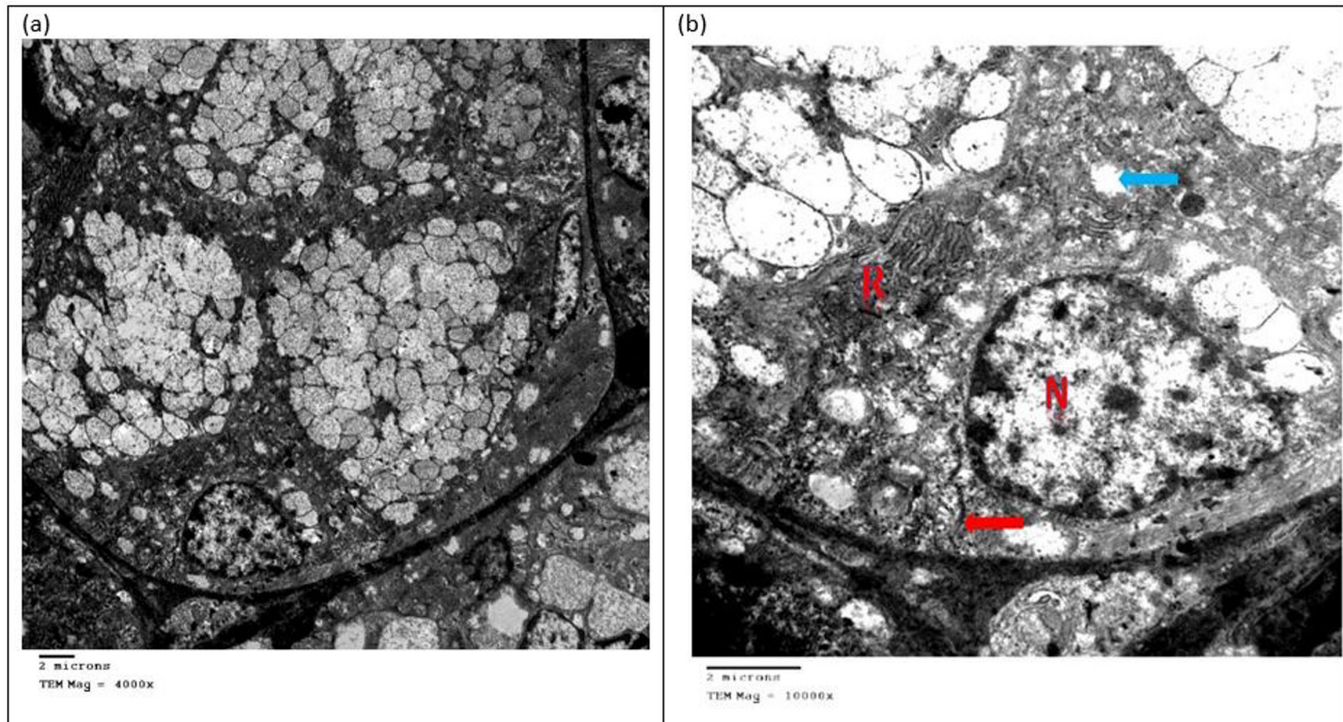


**Fig. 12:** Electron micrograph of acini of submandibular salivary gland of group III showing: [a] acinar cells [b] normally appearing nucleus with prominent nucleolus (N), well organized RER with few dilatation (R), normal mitochondria (red arrow), few damaged mitochondria (blue arrow) (Uranyl acetate and lead citrate [a] x4000 [b] x10000).

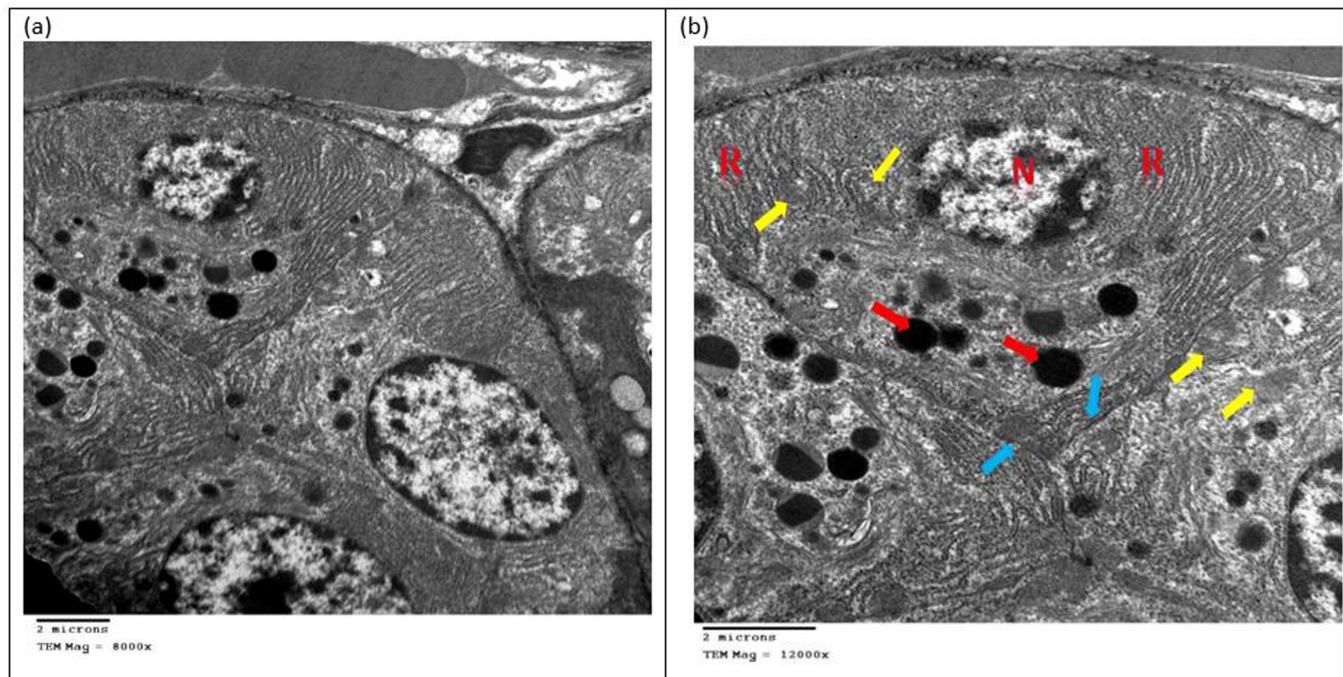


**Fig. 13:** Electron micrograph of intercalated duct of submandibular salivary gland of group III showing: [a] intercalated duct cells [b] normally appearing nucleus (N), normally appearing mitochondria (yellow arrows), uniform slightly dilated RER (R), electron dense secretory granules (red arrows), intercellular junctions (blue arrows) (Uranyl acetate and lead citrate [a] x8000 [b] x12000).

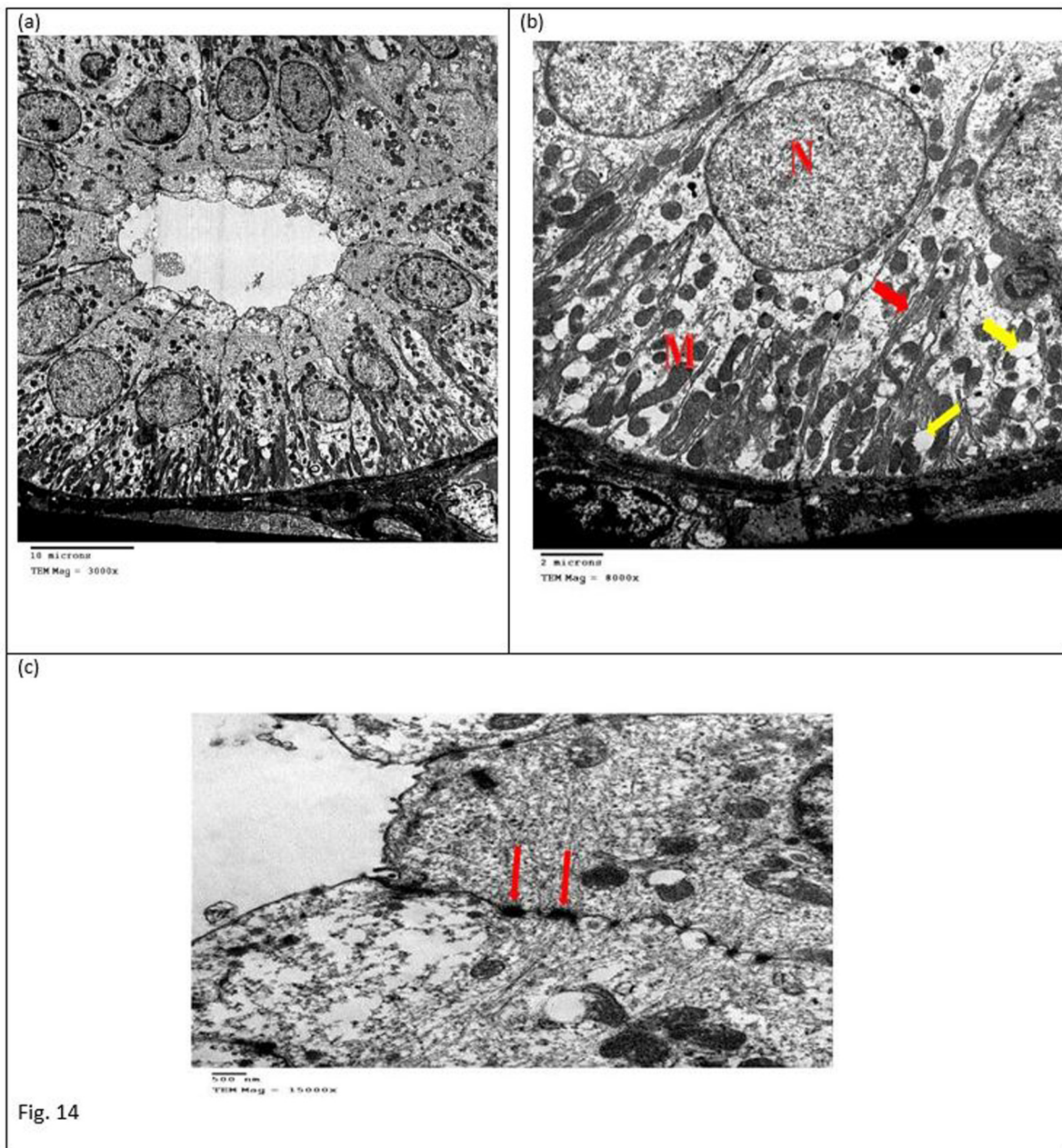


**Fig. 14:** Electron micrograph of striated duct of submandibular salivary gland of group III showing: [a] striated duct cells [b] normal nucleus (N), radial arrangement of mitochondria (M), scanty RER (red arrow), few cytoplasmic vacuolation (yellow arrows) [c] intact intercellular desmosomal junctions (red arrows) (Uranyl acetate and lead citrate [a] x3000 [b] x8000 [c] x15000).

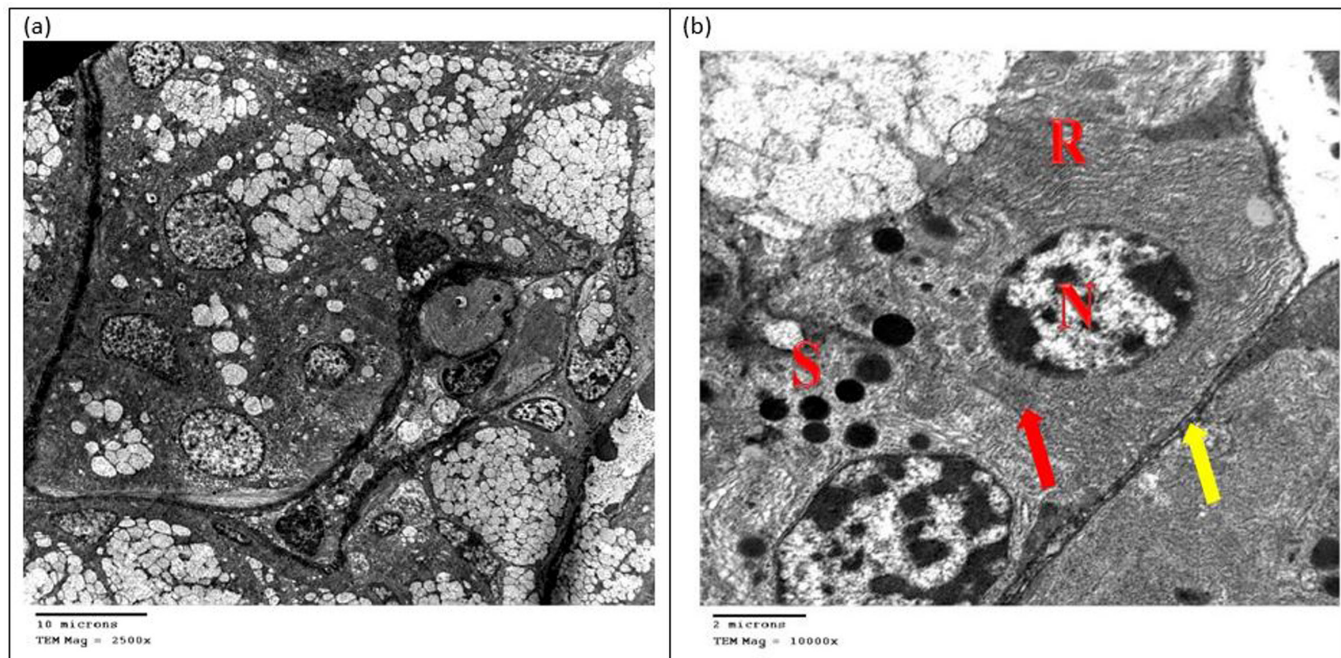


**Fig. 15:** Electron micrograph of GCT of submandibular salivary gland of group III showing: [a] GCT cells [b] normal nucleus (N), electron dense secretory granules (S), normal RER with few distended cisternae (R), normal Mitochondria (red arrow), intact intercellular junctions (yellow arrow) (Uranyl acetate and lead citrate [a] x2500 [b] x10000).

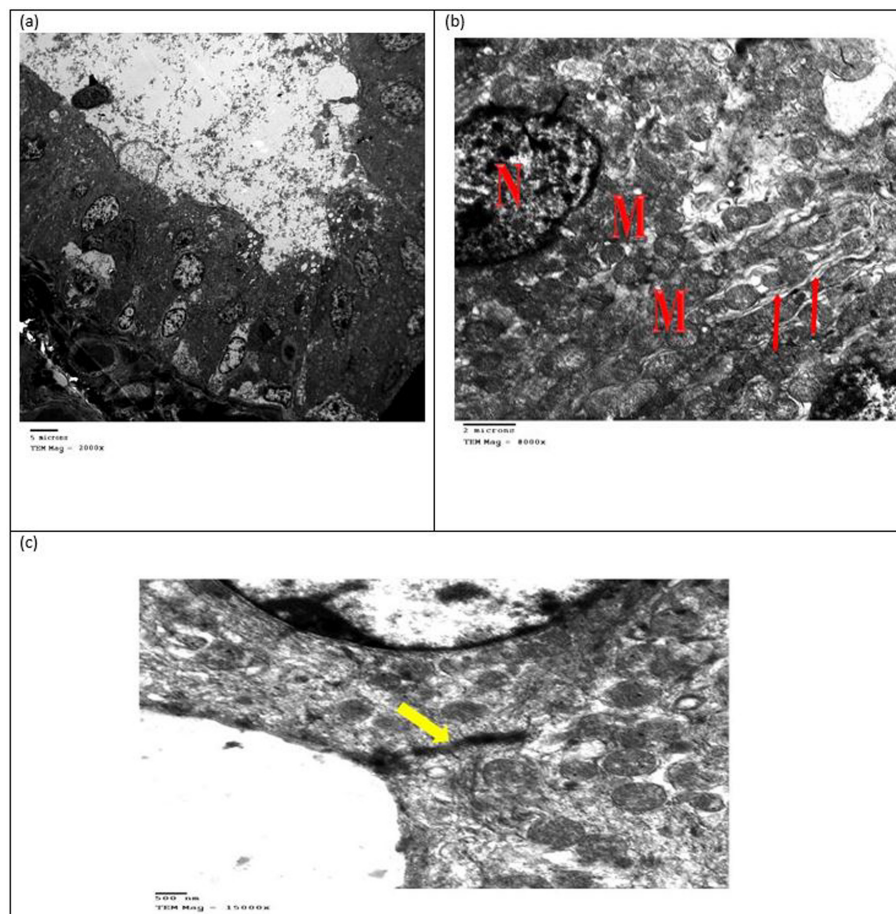


**Fig. 16:** Electron micrograph of excretory duct of submandibular salivary gland of group III showing: [a] excretory duct cells [b] normal nucleus (N), numerous normal mitochondria (M), scanty RER (red arrows) [c] normal desmosomal junction (yellow arrow) (Uranyl acetate and lead citrate [a] x2000 [b] x8000 [c] x15000).

## DISCUSSION

In this research, we aimed to evaluate the effect of BM-MSCs on the histological structure of submandibular salivary gland of carbimazole-induced hypothyroidism in rats by means of transmission electron microscopic (TEM) examination.

The submandibular gland was the gland of choice in this study since rodents' salivary glands show a degree of similarity when compared histologically to human submandibular salivary gland. However, rodent submandibular glands develop GCTs producing a variety of growth factors<sup>[14]</sup>.

According to our research, hypothyroidism was effectively induced by a well known anti-thyroid drug carbimazole. The drug is widely utilized experimentally on animal models<sup>[15]</sup>. Carbimazole reduces the production of thyroid hormones T3 and T4 with subsequent increase in TSH, which comes in agreement with previous investigations<sup>[16]</sup>.

Besides, carbimazole was administered to the animals through a stomach tube. This method was preferable to mixing the drug with diet or with drinking water as the dose could be accurately adjusted<sup>[17]</sup>.

Several workers have suggested that thyroid hormones are important in the maintenance of normal salivary gland function and histology. Therefore, hypothyroidism can cause alterations in the structure and secretory function of the submandibular salivary gland<sup>[18]</sup>.

In our research, acinar and ductal cells of the hypothyroid group (group II) showed early apoptotic changes with pyknotic, irregular nuclei and chromatin condensation. Missarranged dilated RER cisternae together with areas of vacuolar degeneration were also recognized. These data are in harmony with results obtained from previous study which verified that hypothyroidism results in acinar alterations showing nuclear apoptosis, dilatation of RER and numerous cytoplasmic vacuolation in the parotid gland<sup>[19]</sup>. One possible explanation documented that the nucleus acquired irregular forms to increase the surface area of contact with the cytoplasm as it is considered as compensatory mechanism for reduced metabolic activity due to apoptosis<sup>[20]</sup>. However, Shubin *et al.* reported that vacuolation may cause apoptosis or cell death<sup>[21]</sup>. Another study spotted that under electron microscope, vacuolations were damaged organelles such as mitochondria and lysosomes or could be autophagic vacuoles<sup>[13,22]</sup>. Vacuolated areas in the acinar cytoplasm could be also a result of edema replacing degenerated cells, or may be due to fatty degeneration<sup>[22]</sup>. Meanwhile, previous study proved that dilated and disrupted RER could be due to accumulation of iso-osmotic fluid in the cells<sup>[23]</sup>.

As well, TEM examination revealed apparent loss of basal striations in the striated ducts of group II. The mitochondria were markedly distended with massive disruption of their cristae. This finding was parallel to that

described by Ayuob<sup>[1]</sup> who reported that hypothyroidism caused degeneration of salivary glands' mitochondria which appeared swollen with loss of cristae. It is conceivable to suggest that mitochondrial damage could be referred to the cytotoxic property of reactive oxygen species (ROS) that attacks mitochondrial DNA, hence impairing mitochondrial metabolism<sup>[24]</sup>.

All of the previously documented degenerative changes following carbimazole treatment were strongly attributed to the free radical damaging effect resulting from hypothyroidism<sup>[25]</sup>. It is well known that thyroid hormones are important in regulating oxidative metabolism and production of free radicals<sup>[26]</sup>. They also regulate the synthesis and degradation of enzymes, like glutathione peroxidase, glutathione reductase, superoxide dismutase and catalase<sup>[27]</sup>. Experimental studies were conducted to show that low level of thyroid hormones may cause lower metabolic rate and considerable production of free radicals in many tissues. Moreover, the formation of ROS accompanied by hypothyroidism may result in genetic abnormalities and physiological alterations leading to cell death and aging<sup>[28]</sup>.

MSCs were initially isolated from bone marrow. Therefore, BM-MSCs have been the golden standard in MSCs researches<sup>[29]</sup>. MSCs were chosen in this study as they present low degree of immunogenicity, low carcinogenicity following transplantation, have no ethical problems, plus the ease of their collection<sup>[30]</sup>. They also have chemotactic capability which direct them to the damaged tissues<sup>[31]</sup>. In addition, they can proliferate rapidly in culture medium without loss of their differentiation ability<sup>[32]</sup>. They also have relatively short culture time<sup>[33]</sup>. Besides, BM-MSCs can easily isolated and divided into multipotent mesenchymal stromal cells<sup>[34]</sup>.

Intravenous injection of BM-MSCs had been used in this study to trace the labeled BM-MSCs homing in rats' submandibular salivary glands. They circulate in small amounts, then settle in tissues to allow for tissue regeneration and repair<sup>[35]</sup>. It was also found that injectable mechanism avoids the risk of local invasive mechanism<sup>[34]</sup>.

Labeling of BM-MSCs was done, in the herein study, using PKH26 fluorescent dye. This material was selected as it allows rapid labeling without changing proliferation or functions of the cells<sup>[36]</sup>.

In accordance to our research, three weeks after BM-MSCs injection (group III) revealed well defined nuclear membrane with homogenously distributed peripheral chromatin. Well organized normally appearing RER and mitochondria were constant features in both acinar and ductal cells. Furthermore, few electron dense secretory granules and few vacuolated areas were detected with no disruption of cellular junctions.

Similarly, previous results reported that MSCs can restore the acino-ductal architecture following induction of hypothyroidism by their ability to differentiate into salivary

parenchymal cells<sup>[37]</sup>. These data were also in agreement with authors who injected BM-MSCs in irradiated mice and rats. Their results revealed enhanced proliferation and function in the submandibular salivary gland, together with decreased apoptosis and increased vascularity<sup>[38,39]</sup>. Recently, a study reported that systemic injection of BM-MSCs following irradiation could restore 90–100% of salivary flow in irradiated mice<sup>[6]</sup>. Another study showed that intravenous transplantation of BM-MSCs rescued the functional injury of irradiated submandibular glands of mice<sup>[40]</sup>.

Collectively, the improvements detected in group III could be clarified either by the anti-hypothyroid influence of BM-MSCs, consequently inhibiting oxidative stress<sup>[41]</sup>, or by homing of injected BM-MSCs in the submandibular salivary glands<sup>[42,43]</sup>.

Another possible explanation of these obtained data proved the capability of BM-MSCs to inhibit apoptosis. Previous study reported decreased apoptosis and increased proliferation indices causing improvement in renal function after MSCs transplantation in renal ischemia<sup>[44]</sup>. The anti-apoptotic properties of MSCs could be due to the paracrine effect of interleukin – 6 (IL-6) secreted by MSCs which activates signaling pathways that mediate the production of antiapoptotic genes<sup>[39]</sup>. Adding BM-MSCs to damaged salivary glands induced repair process by paracrine enhancement, which allows recovery of the gland's morphology. The paracrine action such as the secretion of anti-inflammatory, anti-apoptotic, proliferating and differentiating promoting factors was found to enhance tissue renewal in several diseases<sup>[6]</sup>.

Also, it has been hypothesized that MSCs can save the damaged tissue through direct cell communication with the formation of intercellular nanotubes with surrounding cells<sup>[45]</sup>. Consequently, dual exchange of their mitochondria occurs through the nanotubes. MSCs could save the damaged tissue through the transport of their healthy mitochondria. Though, the function of the mitochondria transferred from damaged cells to MSCs is unidentified and needs further investigations<sup>[46]</sup>.

Based on the formerly mentioned data, it is conceivable to conclude that BM-MSCs may have the potentiality to ameliorate salivary glands damage of carbimazole induced hypothyroidism. They are also capable to restore the gland's architecture by almost normal appearance of acini and ducts following induction of hypothyroidism.

#### CONFLICT OF INTERESTS

There are no conflicts of interest.

#### REFERENCES

1. Ayuob N: Histological and immunohistochemical study on the possible ameliorating effects of thymoquinone on the salivary glands of rats with experimentally induced hypothyroidism. *EJH*. (2016) 39 (2): 125-35.
2. Hayat N, Tahir M, Munir B and Sami W: Effect of methimazole-induced hypothyroidism on histological characteristics of parotid gland of Albino rats. *J Ayub. Med. Coll. Abbottabad*. (2010) 22 (3): 22-26.
3. Kassab AA and Tawfik SM: Effect of a caffeinated energy drink and its withdrawal on the submandibular salivary gland of adult male albino rats: A histological and immunohistochemical study. *EJH*. (2018) 41 (1): 11-26.
4. Volarevic V, Arsenijevic N, Lukic ML and Stojkovic M: Concise review: mesenchymal stem cell treatment of the complications of diabetes mellitus. *Stem cells*. (2011) 29 (1): 5-10.
5. Sudhakar PJ and Kameswararao PB: Literature review on stem cell treatment & oral submucous fibrosis. *J Evol. Med. Dent Sci*. (2015) 4 (63):11058-11062.
6. Elsaadany B, Zakaria M and Mousa MR: Transplantation of Bone Marrow-Derived Mesenchymal Stem Cells Preserve the Salivary Glands Structure after Head and Neck Radiation in Rats. *Open Access Maced. J Med. Sci*. (2019) 7 (10): 1588-1592.
7. Elsaadany B, El Kholy S, El Roubay D, Rashed L and Shouman T: Effect of Transplantation of Bone Marrow Derived Mesenchymal Stem Cells and Platelets Rich Plasma on Experimental Model of Radiation Induced Oral Mucosal Injury in Albino Rats. *Int. J Dent*. (2017) 2017: 8634540.
8. Hu S, Borrelli M, Lorenz H, Longaker M and Wan D: Mesenchymal Stromal Cells and Cutaneous Wound Healing: A Comprehensive Review of the Background, Role, and Therapeutic Potential. *Stem Cells Int*. (2018) 2018: 6901983.
9. Rashed FM, GabAllah OM, AbuAli SY and Shredah MT: The Effect of Using Bone Marrow Mesenchymal Stem Cells Versus Platelet Rich Plasma on the Healing of Induced Oral Ulcer in Albino Rats. *Int. J stem cells*. (2019) 12 (1): 95-106.
10. Ajayi A, Adalokun A and Akhigbe R: Gastric Mucosa Damage and Impairment of Secondary Immune Response in Dysthyroidism is Associated with TNF- $\alpha$  Expression. *Int. J Biol. Med. Res*. (2017) 8 (3): 6063-6069.
11. Hayat N, Nadir S and Muneera M: The effect of hypothyroidism on the body weight of adult Albino wistar Rats. *JRMC*. (2016) 20 (2): 147-149.
12. Lubis AM, Sandhow L, Lubis VK, Noor A, Gumay F, Merlina M, Yang W, Kusnadi Y, Lorensia V, Sandra, F and Susanto N: Isolation and cultivation of mesenchymal stem cells from iliac crest bone marrow for further cartilage defect management. *Acta. Med. Indones*. (2011) 43 (3):178-184.

13. Singh AD and Singh O: Ultrastructural changes in the sublingual salivary gland of prenatal buffalo (*Bubalus bubalis*). *Vet. World.* (2016) 9 (3):326-329.
14. Amano O, Mizobe K, Bando Y and Sakiyama K: Anatomy and histology of rodent and human major salivary glands-Overview of the japan salivary gland society-sponsored workshop. *Acta. Histochem. cytochem.* (2012) 45 (5): 241-250.
15. Sakr SA, Mahran HA and Nofal AE: Effect of selenium on carbimazole-induced histopathological and histochemical alterations in prostate of albino rats. *Am. J Med. Sc.* (2012) 2 (1):5-11.
16. Al-Shaikh MN, Wahab TA and Abdul SH: Hypothyroidism induced by carbimazole in diabetic mice and its Management Using Parsley and *Eruca sativa* oil. *IOSR-JPBS.* (2014) 9 (1):24-27.
17. Shehata MR, Mohamed DA, El-Meligy MM and Bastwrous AE: The effect of maternal hypothyroidism on the postnatal development of the pituitary–thyroid axis in albino rats: a histological, morphometric, and immunohistochemical study. *J Curr. Med. Res. Prac.* (2017) 2 (1):79-97.
18. Hayat NQ: Effect of Hypothyroidism on the Histology of Sublingual Salivary Gland in Adult Albino Rats. *JRMC.* (2017) 21 (4):395-399.
19. Hassan IZ: Effect of experimentally induced hypothyroidism on the parotid gland of adult male albino rats and the possible role of thyroid hormone supplementation. *Br. J Hist. Sci.* (2016) 14 (1): 19-36.
20. Losito N, Botti G, Lonna F, Pasquinelli G, Minenna P and Bisceglia C: Clear-cell myoepithelial carcinoma of the salivary glands: a clinicopathologic, immunohistochemical, and ultrastructural study of two cases involving the submandibular gland with review of the literature. *Pathology-Research and Practice,* (2008) 204 (5): 335-344.
21. Shubin V, Demidyuk I, Komissarov A, Rafieva L and Kostrov S: Cytoplasmic vacuolization in cell death and survival. *Oncotarget.* (2016) 7 (34): 55863–55889.
22. Duntas LH: Thyroid disease and lipids. *Thyroid.* (2002) 12 (4):287-293.
23. Sharma B: Oxidative stress in HIV patients receiving antiretroviral therapy. *Current HIV research.* (2014) 12 (1):13-21.
24. Hidayat M, Khaliq S, Khurram A and Lone KP: Protective effects of melatonin on mitochondrial injury and neonatal neuron apoptosis induced by maternal hypothyroidism. *Melatonin Res.* (2019) 2 (4):42-60.
25. De Jesus VC, Beanes G, Paraguassú GM, Ramalho LM, Pinheiro AL, Ramalho MJ: Influence of laser photobiomodulation (GaAlAs) on salivary flow rate and histomorphometry of the submandibular glands of hypothyroid rats. *Laser Med. Sci.* (2015) 30 (4): 1275-1280.
26. Mancini A, Di Segni C, Raimondo S, Olivieri G, Silvestrini A: Thyroid hormones, oxidative stress, and inflammation. *Mediat. inflamm.* (2016) 2016: 6757154.
27. Ighodaro OM and Akinloye OA: First line defence antioxidants-superoxide dismutase (SOD), catalase (CAT) and glutathione peroxidase (GPX): Their fundamental role in the entire antioxidant defence grid. *Alexandria J Med.* (2018) 54 (4):287-293.
28. Ajayi A, Adelakun A and Akhigbe R: Gastric Mucosa Damage and Impairment of Secondary Immune Response in Dysthyroidism is Associated with TNF- $\alpha$  Expression. *Int. J Biol. Med. Res.* (2017) 8 (3):6063-6069.
29. Venkataramana NK, Kumar SK, Balaraju S, Radhakrishnan RC, Bansal A, Dixit A, Rao D, Das M, Jan M, Gupta P and Totey S: Open-labeled study of unilateral autologous bone-marrow-derived mesenchymal stem cell transplantation in Parkinson's disease. *Transl. Res.* (2010) 155 (2):62-70.
30. Hu C, Yong X, Li C, Lü M, Liu D, Chen L, Hu J, Teng M, Zhang D, Fan Y and Liang G: CXCL12/ CXCR4 axis promotes mesenchymal stem cell mobilization to burn wounds and contributes to wound repair. *J Surg. Res.* (2013) 183 (1):427-434.
31. Radwan RR and Mohamed HA: *Nigella sativa* oil modulates the therapeutic efficacy of mesenchymal stem cells against liver injury in irradiated rats. *J Photochem. Photobiol. B.* (2018)178:447-456.
32. Abd El-Haleem MR, Selim AO and Attia GM: Bone marrow–derived mesenchymal stem cells ameliorate parotid injury in ovariectomized rats. *Cytotherapy.* (2018) 20 (2):204-217.
33. Fan XL, Zhang Y, Li X and Fu QL: Mechanisms underlying the protective effects of mesenchymal stem cell-based therapy. *Cell Mol. Life Sci.* (2020) 77 (14):2771-2794.
34. Denewar M and Amin LE: Role of bone marrow-derived mesenchymal stem cells on the parotid glands of streptozotocin induced diabetes rats. *J Oral Biol. Craniofac. Res.* (2020) 10:33-37.
35. Aziz MT, El-Asmar MF, Haidara M, Atta HM, Roshdy NK, Rashed LA, Sabry D, Youssef M, Abdel Aziz A and Moustafa M: Effect of bone marrow-derived mesenchymal stem cells on cardiovascular complications in diabetic rats. *Med. Sci. Monit.* (2008) 14 (11):BR249-255.
36. El Sadik AO, El Ghamrawy TA and Abd El-Galil TI: The effect of mesenchymal stem cells and chitosan gel on full thickness skin wound healing in albino rats: histological, immunohistochemical and fluorescent study. *PLoS one.* (2015) 10 (9): e0137544.

37. Lim JY, Yi T, Choi JS, Jang YH, Lee S, Kim HJ, Song S and Kim Y: Intraglandular transplantation of bone marrow-derived clonal mesenchymal stem cells for amelioration of post-irradiation salivary gland damage. *Oral Oncol.* (2013) 49 (2):136-43.
38. Tran SD, Liu Y, Xia D, Maria OM, Khalili S, Wang RW, Quan V, Hu S and Seuntjen J: Paracrine effects of bone marrow soup restore organ function, regeneration, and repair in salivary glands damaged by irradiation. *PLoS One.* (2013) 8 (4): e61632.
39. El Emam HF, Abd El Salam NN and Ghazy SE: Impact of bone marrow stem cells application on the methotrexate induced submandibular salivary gland degenerative changes in albino rats (histological and immunohistochemical study. *Egypt. Dent. J.* (2019) 65 (2):1751-1762.
40. Halloom SI, Farid MH, Mehanny SS and Abdel Hamid HF: Stem Cells and Their Potential Effect on Irradiated Submandibular Salivary Glands in Mice. *ADJ.* (2020) 7 (1): 31-39.
41. Lv SS, Liu G, Wang JP, Wang WW, Cheng J, Sun AL, Liu H, Nie H, Su M and Guan G: Mesenchymal stem cells transplantation ameliorates glomerular injury in streptozotocin-induced diabetic nephropathy in rats via inhibiting macrophage infiltration. *Int. immunopharmacol.* (2013) 17 (2):275-282.
42. Wassef MA, Tork OM, Rashed LA, Ibrahim W, Morsi H and Rabie DM: Mitochondrial dysfunction in diabetic cardiomyopathy: Effect of mesenchymal stem cell with ppar- $\gamma$  agonist or exendin-4. *Exp. Clin. Endocrinol. Diabetes.* (2018) 126 (1):27-38.
43. Hamza AA, Fikry EM, Abdallah W and Amin A: Mechanistic insights into the augmented effect of bone marrow mesenchymal stem cells and thiazolidinediones in streptozotocin-nicotinamide induced diabetic rats. *Sci. Rep.* (2018) 8:9827.
44. Tögel F, Weiss K, Yang Y, Hu Z, Zhang P and Westenfelder C: Vasculotropic, paracrine actions of infused mesenchymal stem cells are important to the recovery from acute kidney injury. *Am. J Physiol. Renal. Physiol.* (2007) 292 (5): F1626–1635.
45. Liu K, Ji K, Guo L, Wu W, Lu H, Shan P and Yan C: Mesenchymal stem cells rescue injured endothelial cells in an *in vitro* ischemia–reperfusion model via tunneling nanotube like structure-mediated mitochondrial transfer. *Microvasc. Res.* (2014) 92:10-18.
46. Mahrouf-Yorgov M, Augeul L, Da Silva C, Jourdan M, Rigolet M and Manin S: Mesenchymal stem cells sense mitochondria released from damaged cells as danger signals to activate their rescue properties. *Cell death differ.* (2017) 24 (7): 1224-1238.

## الملخص العربي

## تأثير الخلايا الجذعية الوسيطة المستخرجة من نخاع العظمي علي البنية التحتية النسيجية للغدة اللعابية تحت الفكية عقب احداث قصور في الغدة الدرقية للجرذان (دراسة بالميكروسكوب الالكتروني)

دينا ماجد الدحراوى<sup>١</sup>، هبة أحمد عدوى<sup>٢</sup>، منى فتحى الديب<sup>١</sup>

<sup>١</sup>قسم بيولوجيا الفم- كلية طب الفم والأسنان- جامعة المستقبل

<sup>٢</sup>قسم بيولوجيا الفم- كلية طب الأسنان- جامعة الأزهر (بنات)

**الخلفية:** قصور الغدة الدرقية هو اضطراب ناتج عن عدم كفاية انتاج هرمونات الغدة الدرقية، مما يؤدي الى انخفاض كلى في متطلبات التمثيل الغذائي للجسم، كما يسبب تشوهات خطيرة. الخلايا الجذعية الوسيطة لديها قدرة عالية على التجديد الذاتي. وبالتالي لديها امكانيات علاجية هائلة لاصلاح الأنسجة.

**الهدف من الدراسة:** هدف هذه الدراسة هو تقييم تأثير الخلايا الجذعية الوسيطة المستخرجة من نخاع العظمي علي البنية التحتية النسيجية للغدة اللعابية تحت الفكية عقب احداث قصور في الغدة الدرقية عن طريق معالجة الجرذان بالكاربامازول.

**طرق الدراسة:** تم استخدام واحد وعشرون من ذكور الجرذان البيضاء وقد تم تقسيم الجرذان بالتساوي إلي ثلاثة مجموعات (سبعة جرذان في كل مجموعة). المجموعة الأولى (الضابطة). المجموعة الثانية (المصابه بقصور الغدة الدرقية): تلقت الجرذان جرعة يومية واحدة من كاربامازول (٥ مجم / ٢٥٠ جم / يوم) لمدة خمس أسابيع و ذلك لاحداث قصور الغدة الدرقية. المجموعة الثالثة (المجموعة المعالجة بالخلايا الجذعية المستخلصة من نخاع العظم): في هذه المجموعة ، تم إحداث قصور في الغدة الدرقية على غرار المجموعة الثانية. تلقت الجرذان جرعة واحدة من الخلايا الجذعية النخاعية المستخلصة من نخاع العظمي ( $1 \times 10^6$  خلية معلقة في محلول ملحي ١ مل) عقب احداث قصور الغدة الدرقية مباشرة. تم التخلص من جميع الجرذان بعد ثمانية أسابيع (خمس أسابيع من احداث قصور الغدة الدرقية + ثلاثة أسابيع من حقن الخلايا الجذعية). تم تحضير عينات الغدة اللعابية تحت الفكية للفحص المجهرى الالكتروني.

**النتائج:** كشفت نتائج البنية التحتية للمجموعة الثانية عن تغييرات تنكسية هائلة داخل نوى وعضيات الخلايا. بالإضافة الى تقطع في روابط الخلايا ببعضها. بالإضافة الى ذلك، تم الكشف عن تحسن ملحوظ في البنية التحتية للخلايا باستخدام الخلايا الجذعية المستخلصة من نخاع العظم في المجموعة الثالثة.

**الخاتمة:** الخلايا الجذعية المستخلصة من نخاع العظم لديها القدرة على اصلاح تلف الغدد اللعابية الناتج عن القصور المستحدث في الغدة الدرقية.